Synthesis and Characterization of Phenothiazine-Isoindigo Copolymers for Photovoltaic Applications

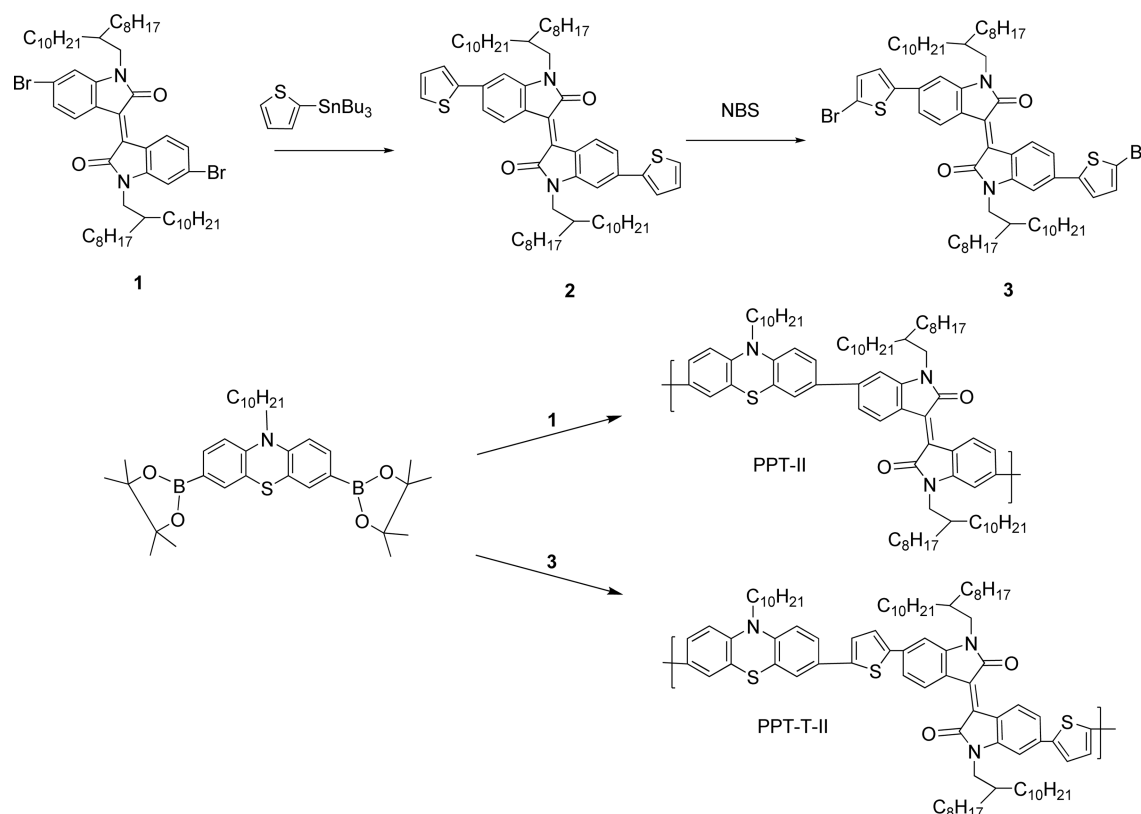**Fuzhen Lyu, Hanok Park, Soo-Hyoung Lee, and Youn-Sik Lee***

*Division of Chemical Engineering, Nanomaterials Processing Research Center, Chonbuk National University, Jeonbuk 561-756, Korea. *E-mail: yosklear@jbnu.ac.kr*

In recent years, polymer solar cells (PSCs) have received a great deal of attention for their low cost, light weight, solution processing capability, and mechanical flexibility.[1,2] The highest PSC power conversion efficiency (PCE) reported in literature is over 8%.[3] The PCE of PSCs is proportional to the short circuit current density (J_{sc}), the open circuit voltage (V_{oc}) and the fill factor (*FF*). The J_{sc} is largely affected by the light-absorption property of *p*-type polymers and the charge mobility of active layers. The V_{oc} is closely related to the energy difference between the highest occupied molecular orbital (HOMO) of a *p*-type conjugated polymer and the lowest unoccupied molecular orbital (LUMO) of an *n*-type material, such as [6,6]-phenyl-C_{71}-butyric acid methyl ester ($PC_{71}BM$). The morphology of the active layer between two electrodes substantially influences the FF value. Thus low band gap polymers with suitable HOMO

and LUMO energy levels should be employed for the fabrication of PSCs with high PCEs.[4]

One of the synthetic strategies for *p*-type polymers involves the combination of electron-donor (D) monomers with electron-acceptor (A) monomers to form alternating D-A polymers. Various D-A polymers have been actively investigated.[5,6] Phenothiazine (PT) is a heterocyclic compound with high electron-donating ability, due to its electron-rich nitrogen and sulfur heteroatoms. Thus PT is an excellent molecular building block to achieve strong donating *p*-type conjugated polymers for photovoltaic devices.[7,8] Recently we reported a PT-diketopyrrolopyrrole polymer (PPT-DPP) with an optical band gap (E^{opt}_g) of 1.63 eV, and a HOMO energy level of −5.20 eV.[9] The PCE of the PPT-DPP-based solar cells was 1.8%. Given this data, if an appropriate acceptor is combined with PT, the resulting copolymer

Scheme 1. Synthetic routes to PPT-II and PPT-T-II.

would still have a low band gap, but a deeper HOMO level, which can increase the V_{oc} and subsequently enhance the PCE. Isoindigo (II), which has a chemical structure similar to that of DPP, has been found to form low band gap polymers with deep HOMO levels,[10-14] leading to increased interest in PT-II copolymers. We attempted to synthesize two different PPT-II copolymers: with (PPT-T-II) or without a thiophene ring (PPT-II) spacer between the PT and II units.

As shown in Scheme 1, PPT-II and PPT-T-II were synthesized from diboronic ester of PT and dibrominated II, both with and without two thiophene rings *via* a Suzuki coupling reaction. PPT-II was readily soluble in common organic solvents such as chloroform, chlorobenzene and *o*-dichlorobenzene, while PPT-T-II was not readily soluble in most organic solvents, with the exception of hot chloroform. The chemical structure of PPT-II was confirmed *via* its proton NMR spectrum (Figure S1). The number-average weights of PPT-II and a soluble portion of PPT-T-II were 55,000 and 7,900 g/mol, and their polydispersion indeces were 1.8 and 1.1, respectively. The low solubility of PPT-T-II may be due to its high molecular weight and/or the increased rigidity of the polymer backbone caused by the unsubstituted thiophene spacers.

The TGA curves of PPT-II and PPT-T-II (Figure S2) show initial 5% weight losses near 350 and 250 °C, respectively. These data indicate that the polymers are thermally stable enough for photovoltaic applications. No thermal transition was observed for the polymers from their DSC experiments in temperatures up to 200 °C. In order to further investigate molecular ordering of the polymers in film, the X-ray diffraction (XRD) patterns of the polymer films were recorded, but no diffraction peak was observed in the 2θ range from 1 to 60°. These results indicate that the polymers are amorphous in nature.

The normalized UV-visible absorption spectra of PPT-II and PPT-T-II in solution and in film are shown in Figure 1. Both polymers show similar absorption spectra: the shorter absorption bands (300-500 nm) correspond to π-π* transitions, and the longer absorption bands (500-700 nm) correspond to intramolecular charge transfer (ICT) between the D
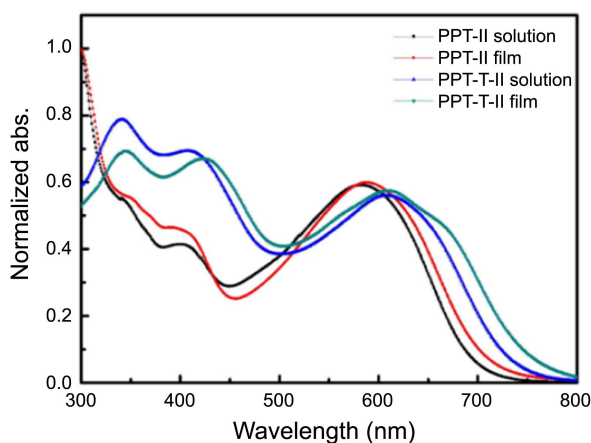
and A units. The maximum absorption wavelengths (λ_{max}s) of PPT-II in solution and in film are 582 and 587 nm, respectively. The relatively small red-shift of the PPT-II film absorption spectrum is probably due to the PT units with a butterfly structure, making intermolecular π-π* interactions difficult. These butterfly-structured PT units may also have caused a small red-shifted spectrum (600 nm in solution versus 607 nm in film) in the PPT-T-II. Compared to PPT-II, the increased coplanarity between the D and A units in PPT-T-II leads to more efficient ICT, which is reflected in the longer λ_{max}.[15] Based on the onset of film absorptions (709 nm for PPT-II and 752 nm for PPT-T-II), the E^{opt}_gs of PPT-II and PPT-T-II were calculated to be 1.75 and 1.65 eV, respectively, indicating that the polymers have relatively low band gaps. The slightly lower band gap of PPT-T-II compared to that of PPT-II is probably due to the thiophene spacer, and the consequently increased coplanarity of PPT-T-II, resulting in more efficient ICT and better π-delocalization.

The onsets of oxidation and reduction potential of PPT-II were 0.93 and −1.19 eV, while those of PPT-T-II were 0.80 and −1.24 eV, respectively (Figure S3). According to an empirical formula, HOMO (eV) = −(E^{ox}_{onset} + 4.4) and LUMO (eV) = −(E^{red}_{onset} + 4.4), the HOMO levels of PPT-II and

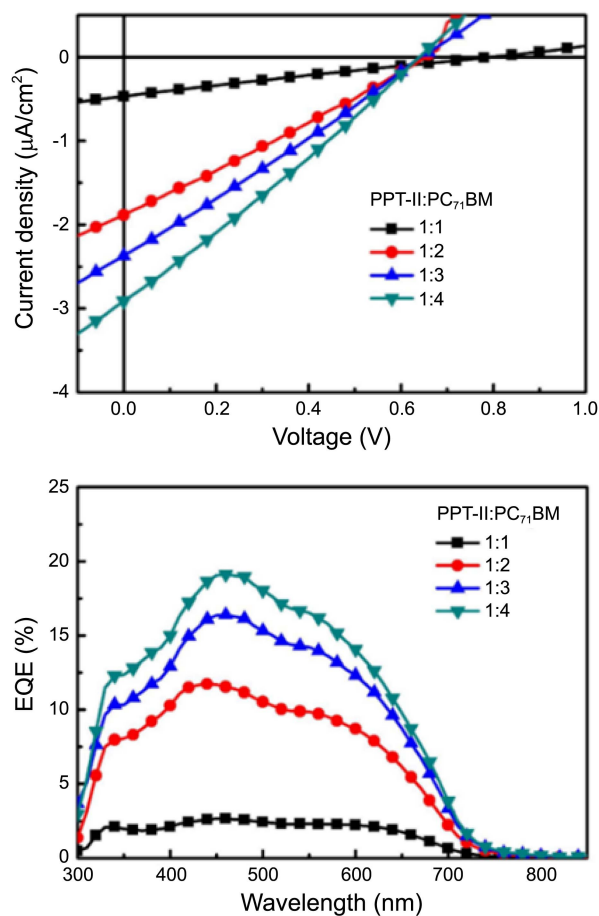**Figure 2.** Current density-voltage (*J-V*) (above) and EQE curves (below) of solar cells with the configuration of ITO/PEDOT:PSS/PPT-II:PC$_{71}$BM/LiF/Al.

Figure 1. Normalized UV-visible absorption spectra of PPT-II and PPT-T-II in chloroform and in film.

PPT-T-II were calculated to be −5.33 and −5.20 eV and their LUMO levels were −3.21 and −3.16 eV, respectively. Thus the electrochemical band gaps (E^{ele}_gs) of PPT-II and PPT-T-II were 2.12 and 2.04 eV, respectively. The E^{ele}_g values for both polymers are greater than the E^{opt}_g values. The discrepancy between the E^{opt}_g and E^{ele}_g values can be attributed to the charge-injection barrier in the interface between the polymer film and electrode.[16] The HOMO level of PPT-T-II is slightly higher than that of PPT-II, probably because both the PT and the thiophene spacer behave as electron-donors.[17] Both the E^{opt}_gs and HOMO levels of these polymers are similar to those of PPT-DPP and PT-quinoxaline polymers (PPT-QX) (E^{opt}_g = 1.76 eV, HOMO = −5.20 eV).[18]

Photovoltaic devices were fabricated using only PPT-II, as PPT-T-II was hardly soluble in most organic solvents. The performances of photovoltaic devices with the configuration ITO/PEDOT:PSS/PPT-II:PC$_{71}$BM/LiF/Al are shown in Figure 2, and their results are summarized in Table 1. As the ratio of PPT-II to PC$_{71}$BM increased from 1:1 to 1:4, the PCE of the devices increased from 0.09 to 0.5%, primarily due to the increasing J_{sc} values. The increased J_{sc} values are probably due to increased light absorption by PC$_{71}$BM and the improved PPT-II/PC$_{71}$BM interface, resulting from the decrease in the domain sizes of the active layer (Figure S4).

The relatively small J_{sc} values may result from the low molar absorptivity of PPT-II, as well as the low charge mobility of the active layers. The small FF values may be due to the low charge mobility of the active layers caused by the butterfly structure of PT moieties. The EQE curves of solar cells indicate that the PCE value increased with the ratio of PPT-II to PCBM, which is consistent with the *J-V* characteristics. The highest EQE values are observed within the range of 450 to 500 nm, though the λ_{max} of PPT-II is near 600 nm. The result suggests that the contribution of PC$_{71}$BM to the PCE is greater than that of the polymer, probably due to a low molar absorptivity for PPT-II. To improve the performance, the devices with an active layer of PPT-II/PC$_{71}$BM (1/4) were thermally annealed. As the annealing temperature increased from 90 to 150 ᵒC, the J_{sc} value increased from 2.9 to 3.9 Am/cm^2 and subsequently the PCE increased from 0.50 to 0.74%, probably due to improved morphology of the active layer. Overall, the device performance of PPT-II is similar to that of PPT-QX (0.83%) but lower than that of PPT-DPP (1.8%).[9,18]

Table 1. Characteristics of the PPT-II-based solar cells

PPT-II :PC$_{71}$BM	Annealing Temp. (ᵒC)	J_{sc} (mA/cm^2)	V_{oc} (V)	*FF* (%)	PCE (%)
1:1	–	0.47	0.79	24	0.09
1:2	–	1.9	0.65	26	0.33
1:3	–	2.4	0.65	26	0.40
1:4	–	2.9	0.64	27	0.50
1:4	90	3.3	0.66	26	0.58
1:4	120	3.6	0.68	26	0.64
1:4	150	3.9	0.70	28	0.74

The molar absorptivity of PPT-II in chloroform was measured to be 1.08×10^3 at 582 nm, significantly less than (36%) that of poly(3-hexylthiophene) (P3HT), a well-known *p*-type polymer (3.02×10^3 at 449 nm). The molar absorptivity of PPT-DPP and PPT-QX were reported to be 80% and 30% that of P3HT, respectively.[9,18] This result supports the hypothesis that the polymer's low molar absorptivity is a primary cause of low PCEs in the photovoltaic devices.

The root mean square (rms) roughness values of PPT-II/PC$_{71}$BM layers with 1:1 and 1:4 ratios shown in the AFM images are 0.91 and 0.30 nm, respectively (Figure S4). It appears that nanostructured domains are slightly more developed in the PPT-II/PC$_{71}$BM (1/4) film. This improved morphology of the active layer may also contribute to the increased performance of the device, which may be reflected in the increased J_{sc} and FF values to some extent. However, the nanostructure of PPT-II/PC$_{71}$BM film is much less developed than that of PPT-DPP/PC$_{71}$BM film.[9]

In summary, two different PT-II copolymers were successfully synthesized, with or without a thiophene spacer between the PT and II units. PPT-II was highly soluble in common organic solvents, while PPT-T-II was not readily soluble due to high molecular weight and/or the presence of unsubstituted thiophene spacers. Both polymers have low optical band gaps (1.65-1.75 eV) with HOMO levels of −5.20 ∼ −5.33 eV. However, PPT-II exhibited a very low molar absorptivity. Furthermore, nanostructured domains in the active layers of PPT-II and PC$_{71}$BM were not clearly observed in the AFM images. Thus the low PCEs of the PPT-II-based solar cells were attributed to the low molar absorptivity of PPT-II and poorly-developed morphology of the active layers.

Experimental

Synthesis. Synthetic procedures for compound 1-3, PPT-II, and PPT-T-II are described in the supporting information.

Measurements. Instruments employed for characterization of the polymers are described in the supporting information.

Fabrication of the Photovoltaic Device. Photovoltaic devices were fabricated with the configuration of ITO/PEDOT:PSS/PPT-II: PC$_{71}$BM/LiF/Al (active area of 9 mm^2). Patterned ITO glasses (2×2 cm) were cleaned ultrasonically in DI water, acetone and isopropyl alcohol, and then treated with UV light and ozone. PEDOT:PSS was spin-coated onto the ITO glass and dried at 90 ᵒC for 20 min under nitrogen. A blend of PPT-II and PC$_{71}$BM in *o*-dichlorobenzene was spin-coated onto the PEDOT: PSS layer for 40 s at 700 rpm. LiF (0.5 nm) and Al (100 nm) layers were deposited *via* thermal evaporation under vacuum (1×10^{-6} torr). The current density-voltage (*J-V*) characteristics of photovoltaic devices were measured in the dark and in white light illumination using an AM 1.5G solar simulator (Newport) at 100 mW/cm^2, adjusted with a standard PV reference cell, (2×2 cm monocrystalline silicon solar cell calibrated at NREL, Colorado, USA) with a Keithley 2400 source-measurement unit. The external quantum efficiency (EQE) was measured using

a Polaronix K3100 spectrometer.

Supporting Information. Synthetic procedures and spectral data are available free of charge on the Web at http://www.csj.jp/journals/bcsj/.

References

1. Kim, J. Y.; Lee, K.; Coates, N. E.; Moses, D.; Nguyen, T. Q.; Dante, M.; Heeger, A. J. *Science* **2007**, *317*, 222.
2. Peet, J.; Kim, J. Y.; Coates, N. E.; Ma, W. L.; Moses, D.; Heeger, A. J.; Bazan, G. C. *Nat. Mater.* **2007**, *6*, 497.
3. Osaka, I.; Kakara, T.; Takemura, N.; Koganezawa, T.; Takimiya, K. *J. Am. Chem. Soc.* **2013**, *135*, 8834.
4. Huo, L.; Hou, J.; Zhang, S.; Chen, H.-Y.; Yang, Y. *Angew. Chem. Int. Ed.* **2010**, *49*, 1500.
5. Li, Y. *Acc. Chem. Res.* **2012**, *45*, 723.
6. Brédas, J.-L.; Norton, J. E.; Cornil, J.; Coropceanu, V. *Acc. Chem. Res.* **2009**, *42*, 1691.
7. Tang, W.; Kietzke, T.; Vemulamada, P.; Chen, Z. *J. Polym. Sci. Part A: Polym. Chem.* **2007**, *45*, 5266.
8. Choi, J.; Lee, B.; Kim, J. H. *Synth. Met.* **2009**, *159*, 1922.
9. Jang, W.; Lyu, F. Z.; Park, H.; Meng, Q. B.; Lee, S.-H.; Lee, Y.-S. *Chem. Phys. Lett.* **2013**, *584*, 119.
10. Wang, T.; Chen, Y.; Bao, X.; Du, Z.; Guo, J.; Wang, N.; Sun, M.; Yang, R. *Dyes Pigm.* **2013**, *98*, 11.
11. Wang, E.; Ma, Z.; Zhang, Z.; Henriksson, P.; Inganas, O.; Zhang, F.; Andersson, M. R. *Chem. Commun.* **2011**, *47*, 4908.
12. Jung, J. W.; Liu, F.; Russell, T. P.; Jo, W. H. *Energ. Environ. Sci.* **2013**, *6*, 3301.
13. Wang, E.; Ma, Z.; Zhang, Z.; Vandewal, K.; Henriksson, P.; Inganas, O.; Zhang, F.; Andersson, M. R. *J. Am. Chem. Soc.* **2011**, *133*, 14244.
14. Xu, X.; Cai, P.; Lu, Y.; Choon, N. S.; Chen, J.; Hu, X.; Ong, B. S. *J. Polym. Sci. Part A: Polym. Chem.* **2013**, *51*, 424.
15. Baek, M.-J.; Lee, S.-H.; Kim, D. H.; Lee, Y.-S. *Macromol. Res.* **2011**, *20*, 147.
16. Jo, M. Y.; Bae, J. H.; Lim, G. E.; Ha, Y. E.; Katz, H. E.; Kim, J. H. *Synth. Met.* **2013**, *176*, 41.
17. Osaka, I.; Zhang, R.; Liu, J.; Smilgies, D.-M.; Kowalewski, T.; McCullough, R. D. *Chem. Mater.* **2010**, *22*, 4191.
18. Jang, W.; Yang, Y. Q.; Kim, J.-S.; Lee, S.-H.; Lee, Y.-S. *Bull. Korean Chem. Soc.* **2013**, *34*, 1887.